

No.54

MAY 2008.

CONTENTS

	pg.
Interbraided Cylindrical Braids	1273

A quarterly publication
for
the braiding artisan

Resale of this publication or copies thereof
is strictly prohibited

Copyright ©2008 by :

{ A.G. Schaake; 21 Sundown Cresc.; Hamilton; New Zealand.
D. Van Tassel; Box 335; Craig, Co 81626-0335; U.S.A.
F.J.M. Masurel; Ganzenzijde 4; 2317 XG Leiden; Nederland.

All rights reserved. No part of this publication may be reproduced, stored in a retrieval system, or transmitted, in any form or by any means, electronic, mechanical, photo-copying, recording, or otherwise, without prior written permission.

This publication is available to braiding artisans only.

Copies may be obtained from :

A.G. Schaake,
21 Sundown Cresc.,
Hamilton,
New Zealand.

Interbraided Cylindrical Braids

In *The Braider*, Issue No. 53, pg. 1265, we introduced a “new” type of Interbraided Cylindrical Braid. The helix angle of the string-run in these braids, when braided over a constant diameter, has a constant value throughout the braid. Example 3 on pg. 1265 furnished an example of such an interbraid which requires three essential strings: one for the foundation knot and one for each of the two interbraided Regular Knots. With $B_c = 3m$ for the foundation knot, where m is odd but not an odd multiple of 11, the essential number of strings for the overall interbraid remains the same. The string-run of the foundation knot in this example was depicted in the upper diagram of Fig. 997, pg. 1267. Let’s now redraw this string-run so that the 18 bights on bight-boundary 1_L are regularly spaced. The bight-index number at the end of the first-return string-run will then be $2 \times 18 + 8 = 36 + 8 = 44$, while $C_1 = C_3 = 9$. Hence $4C_1 + C_2 = 36 + C_2 = 44$, and consequently $C_2 = 8$. This results in the string-run depicted in Fig. 1003.

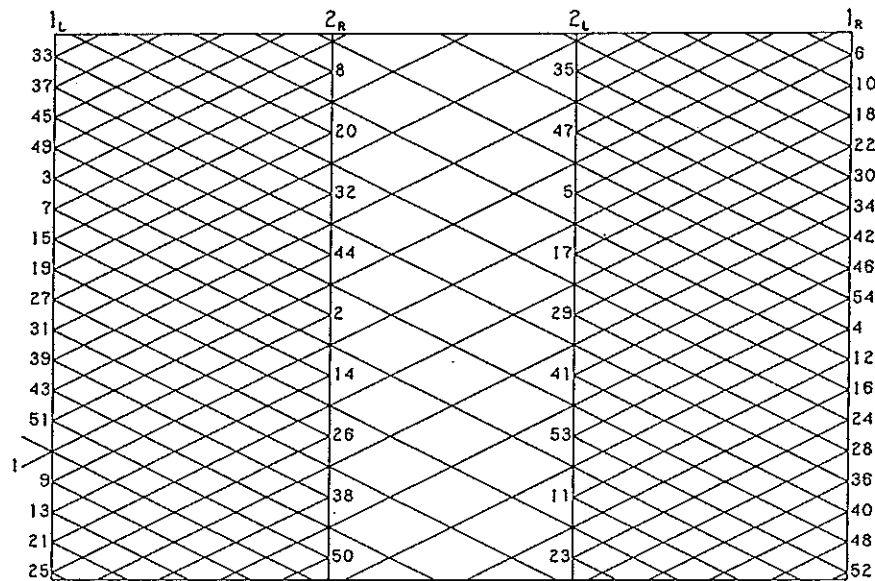


Fig. 1003 — The string-run diagram of the foundation knot.

Note that for the foundation knot in this diagram also $\beta = 66$ and $B_c = 27$.

It will be evident that a first-return string-run dictates that we can also obtain the value for $\lambda = \text{g.c.d.} \left(\frac{\beta}{\alpha}, \frac{B_c}{\alpha} \right)$ from $\text{g.c.d.} \left(\frac{\beta'}{\alpha'}, \frac{B_c'}{\alpha'} \right)$, where α' is the number of bights in the first-return string-run on the circumferential bight-boundary n , β' is the number of bights the first-return string-run spans in the component on the circumferential bight-boundary n , and B_c' is the component’s number of bights on the circumferential bight-boundary n . The first-return string-run starts and ends on the appropriate circumferential bight-boundary n of course.

For bight-boundary 1_L we obtain $\alpha' = 2$, $\beta' = 2 \times 18 + 8 = 44$, and $B_c' = 18$. Hence $\lambda = \text{g.c.d.} \left(\frac{44}{2}, \frac{18}{2} \right) = \text{g.c.d.} (22, 9) = 1$.

For bight-boundary 2_R we obtain $\alpha' = 1$, $\beta' = 2 \times 9 + 4 = 22$, and $B_c' = 9$. Hence $\lambda = \text{g.c.d.} \left(\frac{22}{1}, \frac{9}{1} \right) = \text{g.c.d.} (22, 9) = 1$.

For bight-boundary 2_L we obtain $\alpha' = 1$, $\beta' = 2 \times 9 + 4 = 22$, and $B_c' = 9$. Hence

$$\lambda = \text{g.c.d.} \left(\frac{22}{1}, \frac{9}{1} \right) = \text{g.c.d.} (22, 9) = 1.$$

For bight-boundary 1_R we obtain $\alpha' = 2$, $\beta' = 2 \times 18 + 8 = 44$, and $B_c' = 18$.

Hence $\lambda = \text{g.c.d.} \left(\frac{44}{2}, \frac{18}{2} \right) = \text{g.c.d.} (22, 9) = 1.$

Note that it is simpler to calculate the value for λ with α' , β' and B_c' than with α , β , and B_c .

The foundation knot in Fig. 1003 can be interbraided with a Regular Knot of which the string-run is shown in Fig. 1004. Hence the overall interbraid requires two essential strings: one for the foundation knot and one for the interbraided Regular Knot.

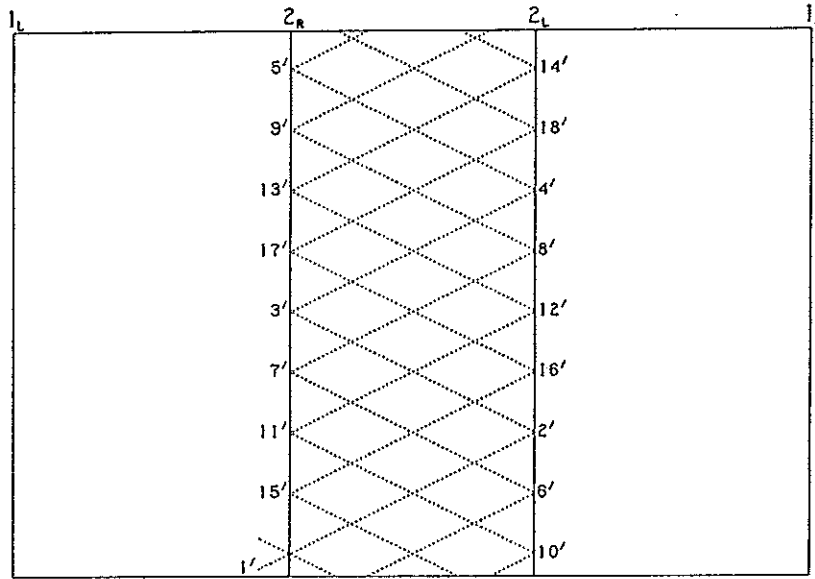


Fig. 1004 — The string-run of the interbraided Regular Knot.

Fig. 1005 shows a coding superimposed on the string-runs of Figs. 1003 and 1004.

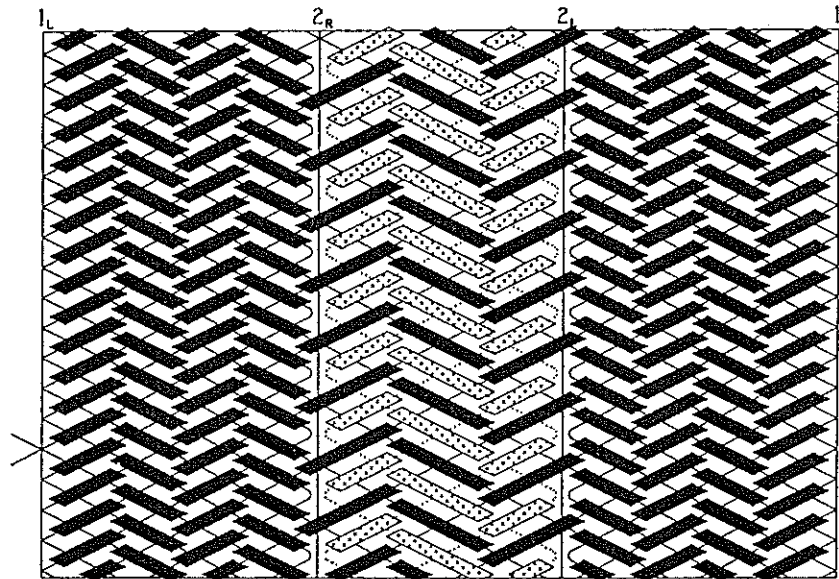


Fig. 1005 — A coding superimposed on the string-runs in Figs. 1003 and 1004.

The half-cycle braiding algorithms for the foundation knot can be read from the tables in Figs. 1006 & 1007. In these tables, half-cycle n intersects the half-cycles

which end at the beginning of the half-cycles $\leq n$ listed on their right. These tables give us the following half-cycle braiding algorithms:

1. $1_L \rightarrow 2_R$: Free run.
2. $2_R \rightarrow 1_L$: Free run.
3. $1_L \rightarrow 1_R$: Free run.
4. $1_R \rightarrow 2_L$: Free run.
5. $2_L \rightarrow 1_R$: Free run.
6. $1_R \rightarrow 1_L$: $u - o$.
7. $1_L \rightarrow 2_R$: o .
8. $2_R \rightarrow 1_L$: o .
9. $1_L \rightarrow 1_R$: $o - u$.
10. $1_R \rightarrow 2_L$: u .
11. $2_L \rightarrow 1_R$: u .
12. $1_R \rightarrow 1_L$: $2u - 2o$.
13. $1_L \rightarrow 2_R$: o .
14. $2_R \rightarrow 1_L$: $2o$.
15. $1_L \rightarrow 1_R$: $3o - 2u$.
16. $1_R \rightarrow 2_L$: $2u$.
17. $2_L \rightarrow 1_R$: $2u$.
18. $1_R \rightarrow 1_L$: $4u - 2o - u$.

HALF-CYCLE								
1	51	43	39	31	27	19	15	7
7	3	49	45	37	33	25	21	13
13	9	X	51	43	39	31	27	19
19	15	7	3	49	45	37	33	25
25	21	13	9	X	51	43	39	31
31	27	19	15	7	3	49	45	37
37	33	25	21	13	9	X	51	43
43	39	31	27	19	15	7	3	49
49	45	37	33	25	21	13	9	X
	0	0	U	U	0	0	U	U

HALF-CYCLE								
5	X	47	43	35	31	23	19	11
11	7	53	49	41	37	29	25	17
17	13	5	X	47	43	35	31	23
23	19	11	7	53	49	41	37	29
29	25	17	13	5	X	47	43	35
35	31	23	19	11	7	53	49	41
41	37	29	25	17	13	5	X	47
47	43	35	31	23	19	11	7	53
53	49	41	37	29	25	17	13	5
	U	U	0	0	U	U	0	0

HALF-CYCLE																					
3	49	45	37	33	25	21	13	9	X	43	31	19	7	53	49	41	37	29	25	17	13
9	X	51	43	39	31	27	19	15	7	49	37	25	13	5	X	47	43	35	31	23	19
15	7	3	49	45	37	33	25	21	13	X	43	31	19	11	7	53	49	41	37	29	25
21	13	9	X	51	43	39	31	27	19	7	49	37	25	17	13	5	X	47	43	35	31
27	19	15	7	3	49	45	37	33	25	13	X	43	31	23	19	11	7	53	49	41	37
33	25	21	13	9	X	51	43	39	31	19	7	49	37	29	25	17	13	5	X	47	43
39	31	27	19	15	7	3	49	45	37	25	13	X	43	35	31	23	19	11	7	53	49
45	37	33	25	21	13	9	X	51	43	31	19	7	49	41	37	29	25	17	13	5	X
51	43	39	31	27	19	15	7	3	49	37	25	13	X	47	43	35	31	23	19	11	7
	0	0	U	U	0	0	U	U	0	0	U	0	0	U	U	0	0	U	U	0	0

Fig. 1006 — Tables for the odd-numbered half-cycles.

19. $1_L \rightarrow 2_R$: $2o - u$.
20. $2_R \rightarrow 1_L$: $2o - u$.
21. $1_L \rightarrow 1_R$: $4o - 2u - o$.

- 22. $1_R \rightarrow 2_L : 2u - o.$
- 23. $2_L \rightarrow 1_R : 2u - o.$
- 24. $1_R \rightarrow 1_L : 2u - o - 2u - 2o - 2u.$
- 25. $1_L \rightarrow 2_R : 2o - u.$
- 26. $2_R \rightarrow 1_L : 2o - 2u.$
- 27. $1_L \rightarrow 1_R : 2o - 2u - 2o - 2u - 2o.$
- 28. $1_R \rightarrow 2_L : 2u - 2o.$
- 29. $2_L \rightarrow 1_R : 2u - 2o.$
- 30. $1_R \rightarrow 1_L : 2u - 2o - 2u - 3o - 2u - o.$
- 31. $1_L \rightarrow 2_R : 2o - 2u - o.$
- 32. $2_R \rightarrow 1_L : 2o - 2u - o.$
- 33. $1_L \rightarrow 1_R : 2o - 2u - 2o - 3u - 2o - u.$
- 34. $1_R \rightarrow 2_L : 2u - 2o - u.$
- 35. $2_L \rightarrow 1_R : 2u - 2o - u.$
- 36. $1_R \rightarrow 1_L : 2u - 2o - 3u - 3o - 2u - 2o.$
- 37. $1_L \rightarrow 2_R : 2o - 2u - o.$
- 38. $2_R \rightarrow 1_L : 2o - 2u - 2o.$
- 39. $1_L \rightarrow 1_R : 2o - 2u - 4o - 3u - 2o - 2u.$
- 40. $1_R \rightarrow 2_L : 2u - 2o - 2u.$

HALF-CYCLE								
2	52	44	40	32	28	20	16	8
8	4	50	46	38	34	26	22	14
14	10	2	52	44	40	32	28	20
20	16	8	4	50	46	38	34	26
26	22	14	10	2	52	44	40	32
32	28	20	16	8	4	50	46	38
38	34	26	22	14	10	2	52	44
44	40	32	28	20	16	8	4	50
50	46	38	34	26	22	14	10	2
	0	0	U	U	0	0	U	U

HALF-CYCLE								
4	54	46	42	34	30	22	18	10
10	6	52	48	40	36	28	24	16
16	12	4	54	46	42	34	30	22
22	18	10	6	52	48	40	36	28
28	24	16	12	4	54	46	42	34
34	30	22	18	10	6	52	48	40
40	36	28	24	16	12	4	54	46
46	42	34	30	22	18	10	6	52
52	48	40	36	28	24	16	12	4
	U	U	0	0	U	U	0	0

HALF-CYCLE																					
6	52	48	40	36	28	24	16	12	4	46	34	22	10	2	52	44	40	32	28	20	16
12	4	54	46	42	34	30	22	18	10	52	40	28	16	8	4	50	46	38	34	26	22
18	10	6	52	48	40	36	28	24	16	4	46	34	22	14	10	2	52	44	40	32	28
24	16	12	4	54	46	42	34	30	22	10	52	40	28	20	16	8	4	50	46	38	34
30	22	18	10	6	52	48	40	36	28	16	4	46	34	26	22	14	10	2	52	44	40
36	28	24	16	12	4	54	46	42	34	22	10	52	40	32	28	20	16	8	4	50	46
42	34	30	22	18	10	6	52	48	40	28	16	4	46	38	34	26	22	14	10	2	52
48	40	36	28	24	16	12	4	54	46	34	22	10	52	44	40	32	28	20	16	8	4
54	46	42	34	30	22	18	10	6	52	40	28	16	4	50	46	38	34	26	22	14	10
	U	U	0	0	U	U	0	0	U	U	0	U	U	0	0	U	U	0	0	U	U

Fig. 1007 — Tables for the even-numbered half-cycles.

- 41. $2_L \rightarrow 1_R : 2u - 2o - 2u.$
- 42. $1_R \rightarrow 1_L : 2u - 2o - 4u - o - u - 2o - 2u - 2o - u.$
- 43. $1_L \rightarrow 2_R : 2o - 2u - 2o - u.$
- 44. $2_R \rightarrow 1_L : 2o - 2u - 2o - u.$

- 45. $1_L \longrightarrow 1_R : 2o - 2u - 4o - u - o - 2u - 2o - 2u - o.$
- 46. $1_R \longrightarrow 2_L : 2u - 2o - 2u - o.$
- 47. $2_L \longrightarrow 1_R : 2u - 2o - 2u - o.$
- 48. $1_R \longrightarrow 1_L : 2u - 2o - 2u - o - 2u - o - u - 2o - 2u - 2o - 2u.$
- 49. $1_L \longrightarrow 2_R : 2o - 2u - 2o - u.$
- 50. $2_R \longrightarrow 1_L : 2o - 2u - 2o - 2u.$
- 51. $1_L \longrightarrow 1_R : 2o - 2u - 2o - 2u - 2o - u - o - 2u - 2o - 2u - 2o.$
- 52. $1_R \longrightarrow 2_L : 2u - 2o - 2u - 2o.$
- 53. $2_L \longrightarrow 1_R : 2u - 2o - 2u - 2o.$
- 54. $1_R \longrightarrow 1_L : 2u - 2o - 2u - 2o - 2u - o - 2u - 2o - 2u - 2o - 2u.$

Note that the entries in the body of the tables in Figs. 1006 & 1007 are identical to the entries in the body of the tables in Figs. 999 & 1000; it are only the coding entries which differ.

Euclid's algorithm, the path formula, the path in the RKT for the interbraided Regular Knot and its associated algorithm diagram are shown in Fig. 1008. For the interbraided Regular Knot (between the bight-boundaries 2_R and 2_L) we read the following half-cycle braiding algorithms from its algorithm diagram:

- 1'. $\quad \quad \quad :$ $o - 2u - o.$
- 2'. $(i = 0) :$ $u - 2o - u.$
- 3'. $(i = 0) :$ $o - 2u - o.$
- 4'. $(i \leq 1) :$ $u - 2o - u.$
- 5'. $(i \leq 1) :$ $o - 2u - o.$
- 6'. $(i \leq 2) :$ $2u - 2o - u.$
- 7'. $(i \leq 2) :$ $2o - 2u - o.$
- 8'. $(i \leq 3) :$ $2u - 2o - u.$
- 9'. $(i \leq 3) :$ $2o - 2u - o.$
- 10'. $(i \leq 4) :$ $2u - 3o - u.$
- 11'. $(i \leq 4) :$ $2o - 3u - o.$
- 12'. $(i \leq 5) :$ $2u - 3o - u.$
- 13'. $(i \leq 5) :$ $2o - 3u - o.$
- 14'. $(i \leq 6) :$ $2u - 3o - 2u.$
- 15'. $(i \leq 6) :$ $2o - 3u - 2o.$
- 16'. $(i \leq 7) :$ $2u - 3o - 2u.$
- 17'. $(i \leq 7) :$ $2o - 3u - 2o.$
- 18'. $(i \leq 8) :$ $2u - 3o - 2u.$

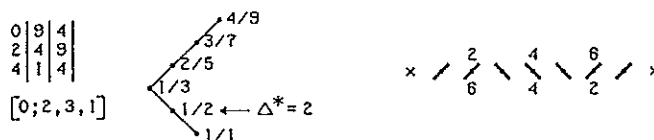


Fig. 1008 — Euclid's algorithm, path formula, path in RKT and algorithm diagram for interbraided Regular Knot.

Let the first-return string-run of a component in a cylindrical braid be as shown in Fig. 1009. In this diagram the bight-index numbers associated with the intersection points between the first-return string-run and the bight-boundaries are indicated. Thus for this component $\beta = 2C_1 + 3C_2 + 2C_3$ while $\alpha = 3$. Let's take $C_1 = C_3$, then $\beta = 4C_1 + 3C_2 = 4C_3 + 3C_2$.

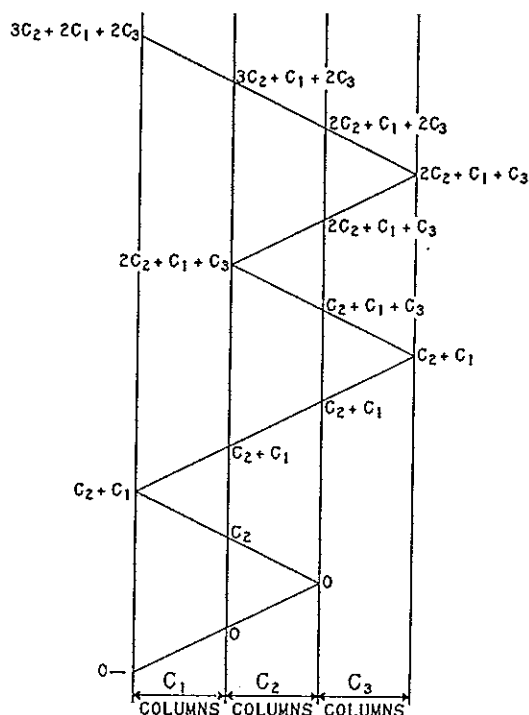


Fig. 1009 — The first-return string-run of a component in a cylindrical braid.

Example 1.

Let $C_1 = C_3 = 15$ and $C_2 = 10$, then $\beta = 4 \times 15 + 3 \times 10 = 90$. Note that C_1, C_2 and C_3 must be chosen so that β is divisible by $\alpha = 3$.

Let $B_c = 21$. Note that B_c must be chosen so that B_c is divisible by $\alpha = 3$.

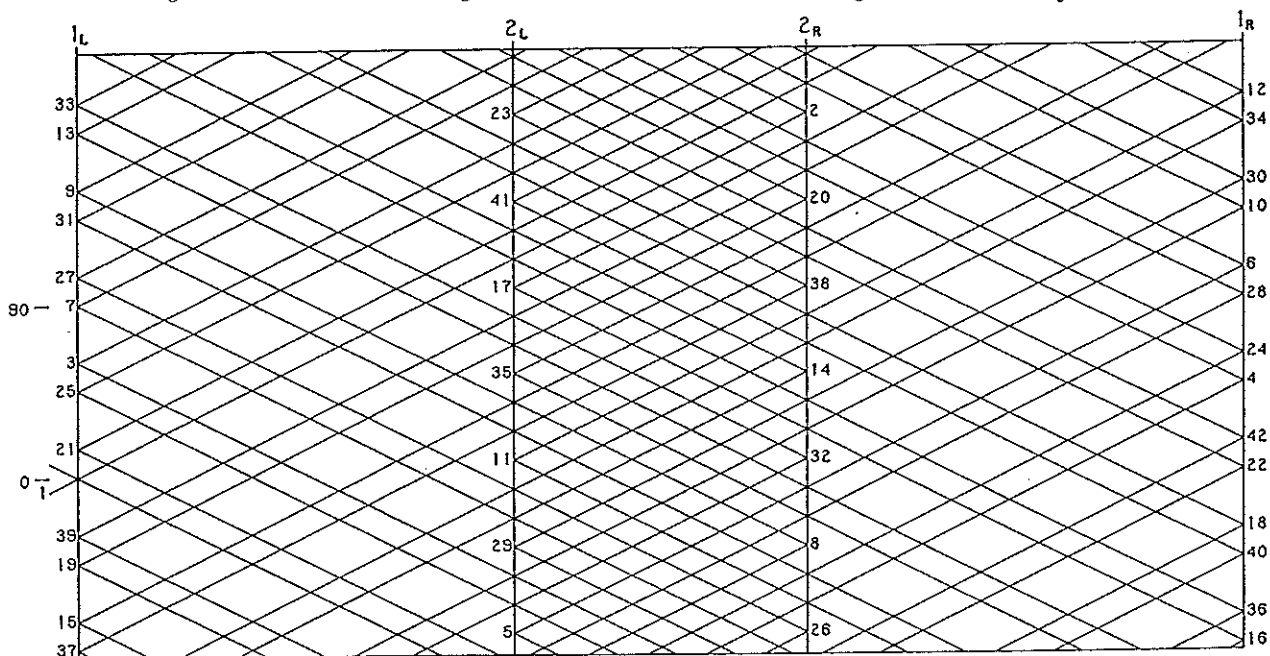


Fig. 1010 — The string-run of the foundation braid.

Thus for this component we obtain:

$$\lambda = \text{g.c.d.} \left(\frac{\beta}{\alpha}, \frac{B_c}{\alpha} \right) = \text{g.c.d.} \left(\frac{90}{3}, \frac{21}{3} \right) = \text{g.c.d.} (30, 7) = 1,$$

and hence only one essential string is required.

The string-run of this component consist of $\left(\frac{B_c}{\alpha}\right) = \left(\frac{21}{3}\right) = 7$ consecutive first-return string-runs.

The diagram in Fig. 1010 depicts the string-run of the foundation braid.

This foundation braid can be interbraided with two Regular Cylindrical Braids, one between the two leftmost bight-boundaries and one between the two rightmost bight-boundaries. For each of these two Regular Cylindrical Braids $p = 5$ and $b = 7$. Hence each braid is a Regular Knot and thus requires only one essential string.

Fig. 1011 depicts the string-runs of the two interbraided Regular Knots.

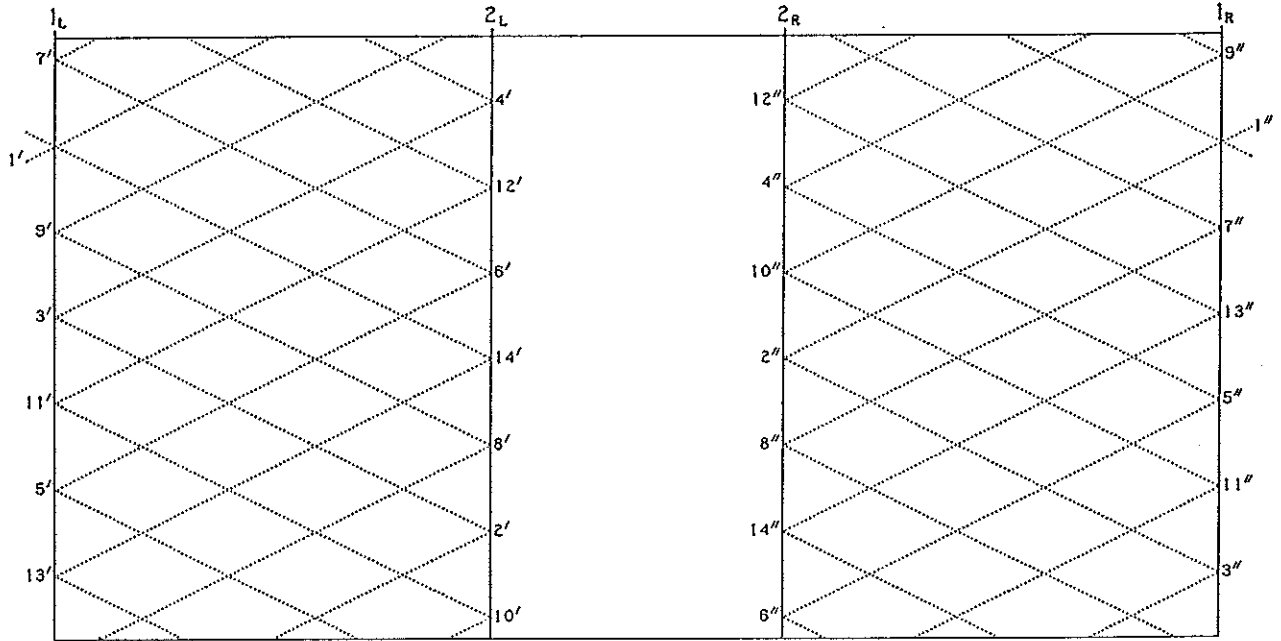


Fig. 1011 — The string-runs of the two interbraided Regular Knots.

A superimposed coding on the three string-runs is shown in Fig. 1012.

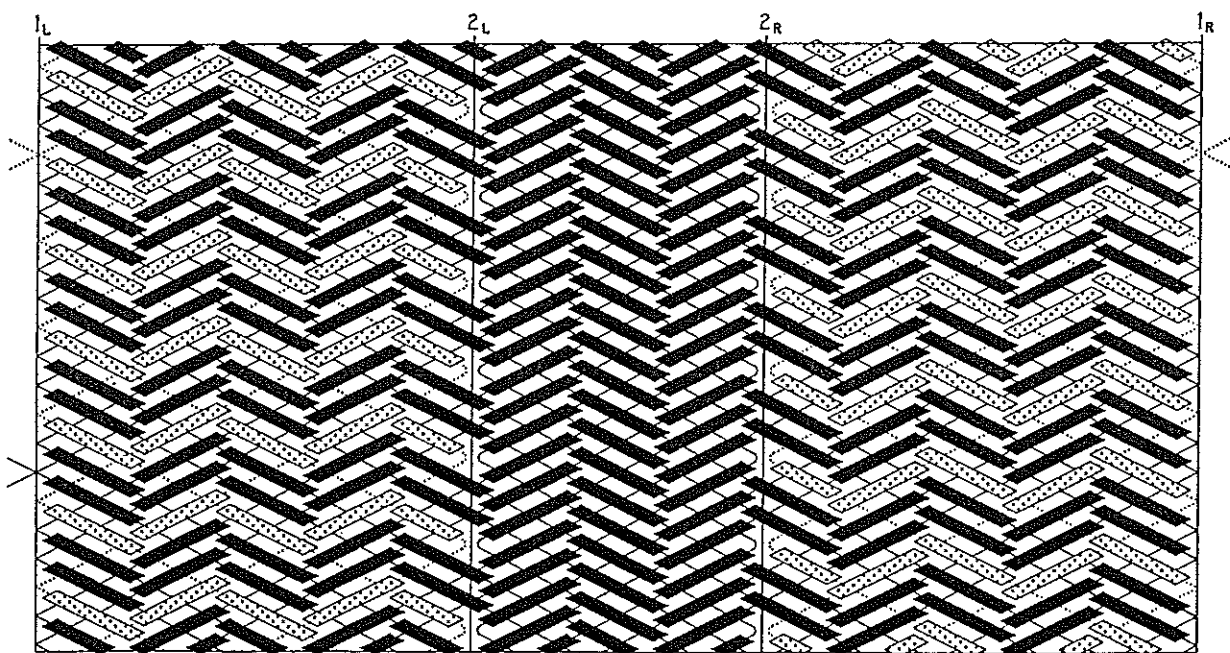


Fig. 1012 — A coding superimposed on the string-runs.

- 30. $1_R \longrightarrow 1_L : o - u - o - u - 2o - 3u - 2o - 2u - o - u - 2o - 2u - 2o.$
- 31. $1_L \longrightarrow 2_R : 6u - 3o - 3u - 2o.$
- 32. $2_R \longrightarrow 1_L : 3u - o - 2u - o - 2u - 2o - 2u - 2o.$
- 33. $1_L \longrightarrow 1_R : u - o - u - 2o - 2u - 3o - 2u - 2o - u - o - 2u - 2o - 2u.$
- 34. $1_R \longrightarrow 2_L : 4o - u - 2o - 3u - 3o - 2u.$
- 35. $2_L \longrightarrow 1_R : 3o - u - 2o - u - 2o - 2u - 2o - 2u.$
- 36. $1_R \longrightarrow 1_L : o - u - 2o - 2u - 2o - 3u - 2o - 2u - 2o - 2u - 2o - 2u - 2o.$
- 37. $1_L \longrightarrow 2_R : 4u - 2o - 2u - 3o - 3u - 2o.$
- 38. $2_R \longrightarrow 1_L : 3u - 2o - 2u - 2o - 2u - 2o - 2u - 2o.$
- 39. $1_L \longrightarrow 1_R : u - 2o - 2u - 2o - 2u - 3o - 2u - 2o - 2u - 2o - 2u - 2o - 2u.$
- 40. $1_R \longrightarrow 2_L : 2o - u - 2o - 2u - 2o - 3u - 3o - 3u.$
- 41. $2_L \longrightarrow 1_R : 3o - 2u - 3o - 2u - 2o - 2u - 2o - 2u.$
- 42. $1_R \longrightarrow 1_L : 2o - 2u - 2o - 2u - 2o - 3u - 3o - 3u - 2o - 2u - 2o - 2u - 2o.$

Euclid's algorithm, the path formula, the path in the RKT for the interbraided Regular Knots and their algorithm diagrams are shown in Fig. 1015.

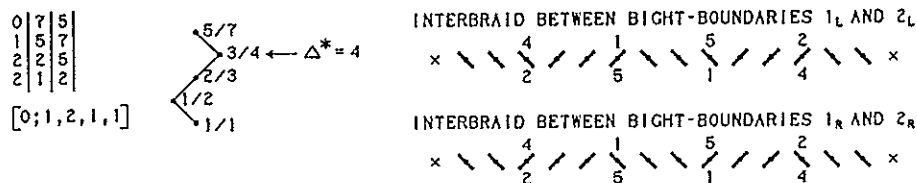


Fig. 1015 — Euclid's algorithm, path formula, path in RKT and algorithm diagrams for interbraided Regular Knots.

For the interbraided Regular Knot between the bight-boundaries 1_L and 2_L we read the following half-cycle braiding algorithms from its algorithm diagram:

- 1'. $2u - 2o - 2u - 2o - 2u.$
- 2'. ($i = 0$) $: 2o - 2u - 2o - 2u - 2o.$
- 3'. ($i = 0$) $: 2u - 2o - 2u - 2o - 2u.$
- 4'. ($i \leq 1$) $: 2o - 2u - 3o - 2u - 2o.$
- 5'. ($i \leq 1$) $: 2u - 3o - 2u - 2o - 2u.$
- 6'. ($i \leq 2$) $: 2o - 2u - 3o - 2u - 3o.$
- 7'. ($i \leq 2$) $: 2u - 3o - 2u - 3o - 2u.$
- 8'. ($i \leq 3$) $: 2o - 2u - 3o - 2u - 3o.$
- 9'. ($i \leq 3$) $: 2u - 3o - 2u - 3o - 2u.$
- 10'. ($i \leq 4$) $: 2o - 3u - 3o - 2u - 3o.$
- 11'. ($i \leq 4$) $: 3u - 3o - 2u - 3o - 2u.$
- 12'. ($i \leq 5$) $: 2o - 3u - 3o - 3u - 3o.$
- 13'. ($i \leq 5$) $: 3u - 3o - 3u - 3o - 2u.$
- 14'. ($i \leq 6$) $: 2o - 3u - 3o - 3u - 3o.$

The half-cycle braiding algorithms for the half-cycles 1''-14'' of the interbraided Regular Knot between the bight-boundaries 1_R and 2_R are identical to the ones above for the half-cycles 1'-14' of the interbraided Regular Knot between the bight-boundaries 1_L and 2_L .

Example 2.

A further two coding arrangements on the string-runs in Figs.1010 and 1011 are depicted in Figs.1016 and 1017.

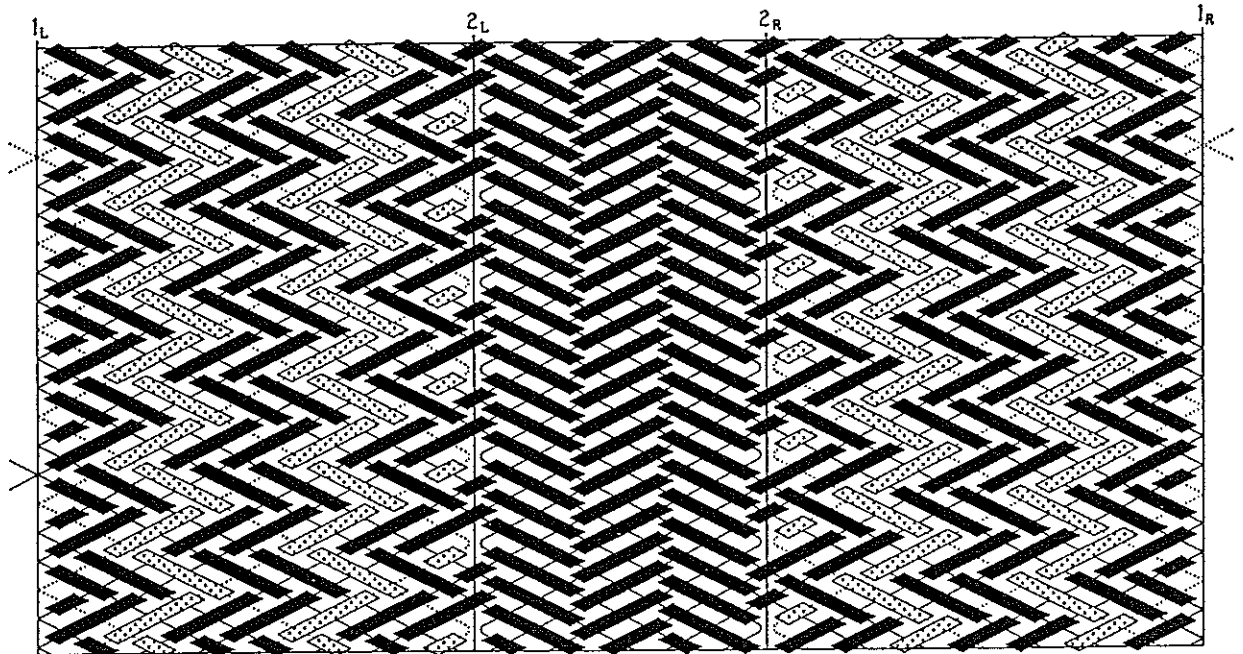


Fig.1016 — An alternative coding arrangement on the string-runs in Figs.1010 and 1011.

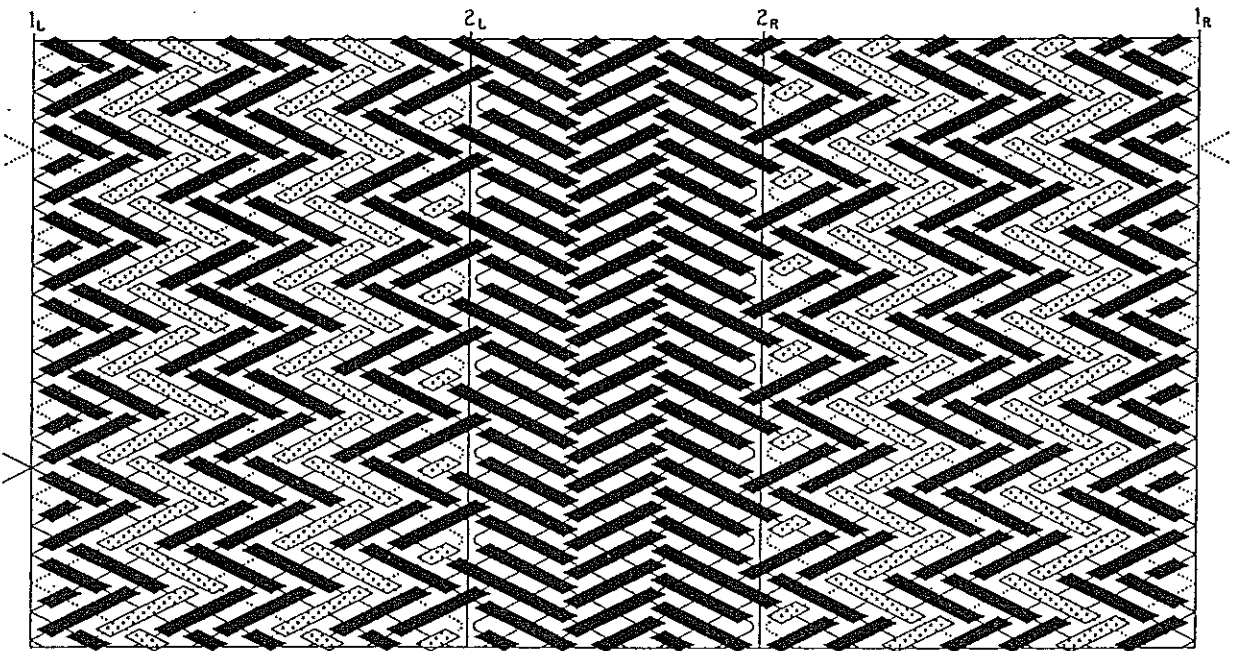


Fig.1017 — An alternative coding arrangement on the string-runs in Figs.1010 and 1011.

The half-cycle braiding algorithms for the foundation braid in Fig.1016 are read from the tables in Figs.1018 & 1019, and are as follows:

1. $1_L \rightarrow 2_R$: Free run.
2. $2_R \rightarrow 1_L$: o .
3. $1_L \rightarrow 1_R$: o .
4. $1_R \rightarrow 2_L$: $o - u$.
5. $2_L \rightarrow 1_R$: $2u$.

- 39. $1_L \longrightarrow 1_R : u - 2o - 2u - 2o - u - o - 3u - 2o - 2u - o - u - 2o - 2u - 2o - 2u.$
- 40. $1_R \longrightarrow 2_L : u - o - 2u - 2o - 3u - 3o - 3u - 3o.$
- 41. $2_L \longrightarrow 1_R : 3u - 2o - 3u - 2o - 2u - 2o - 2u - 2o.$
- 42. $1_R \longrightarrow 1_L : o - 2u - 2o - 2u - 2o - u - 3o - 3u - 3o - u - 2o - 2u - 2o - 2u - o.$

Euclid's algorithm, the path formula, the path in the RKT for the interbraided Regular Knots and their algorithm diagrams are shown in Fig. 1020.

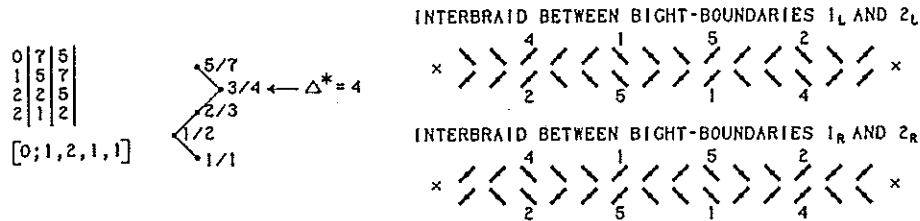


Fig. 1020 — Euclid's algorithm, path formula, path in RKT and algorithm diagrams for interbraided Regular Knots.

For the interbraided Regular Knot between the bight-boundaries 1_L and 2_L we read the following half-cycle braiding algorithms from its algorithm diagram :

- 1'. $2u - 2o - 2u - 2o - u - o.$
- 2'. ($i = 0$) $: 2u - 2o - 2u - 2o - 2u.$
- 3'. ($i = 0$) $: 2u - 2o - 2u - 2o - u - o.$
- 4'. ($i \leq 1$) $: 2u - 2o - 3u - 2o - 2u.$
- 5'. ($i \leq 1$) $: 2u - 2o - 3u - 2o - u - o.$
- 6'. ($i \leq 2$) $: 2u - 2o - 3u - 2o - 3u.$
- 7'. ($i \leq 2$) $: 2u - 2o - 3u - 2o - 2u - o.$
- 8'. ($i \leq 3$) $: 2u - 2o - 3u - 2o - 3u.$
- 9'. ($i \leq 3$) $: 2u - 2o - 3u - 2o - 2u - o.$
- 10'. ($i \leq 4$) $: 2u - 3o - 3u - 2o - 3u.$
- 11'. ($i \leq 4$) $: 2u - 3o - 3u - 2o - 2u - o.$
- 12'. ($i \leq 5$) $: 2u - 3o - 3u - 3o - 3u.$
- 13'. ($i \leq 5$) $: 2u - 3o - 3u - 3o - 2u - o.$
- 14'. ($i \leq 6$) $: 2u - 3o - 3u - 3o - 3u.$

The half-cycle braiding algorithms for the half-cycles 1''-14'' of the interbraided Regular Knot between the bight-boundaries 1_R and 2_R are identical to the ones above for the half-cycles 1'-14' of the interbraided Regular Knot between the bight-boundaries 1_L and 2_L .

The half-cycle braiding algorithms for the foundation braid in Fig. 1017 are read from the tables in Figs. 1021 & 1022, and are as follows :

- 1. $1_L \longrightarrow 2_R : \text{Free run.}$
- 2. $2_R \longrightarrow 1_L : o.$
- 3. $1_L \longrightarrow 1_R : o.$
- 4. $1_R \longrightarrow 2_L : o - u.$
- 5. $2_L \longrightarrow 1_R : 2u.$
- 6. $1_R \longrightarrow 1_L : o - u - 2o.$
- 7. $1_L \longrightarrow 2_R : u - 2o.$
- 8. $2_R \longrightarrow 1_L : 2o - u - o.$

- 41. $2_L \rightarrow 1_R : 3u - 2o - 3u - 2o - 2u - 2o - 2u - 2o.$
- 42. $1_R \rightarrow 1_L : o - 2u - 2o - 2u - 2o - u - 3o - 3u - 3o - u - 2o - 2u - 2o - 2u - o.$

Euclid's algorithm, the path formula, the path in the RKT for the interbraided Regular Knots and their algorithm diagrams are shown in Fig. 1020. Hence the half-cycle braiding algorithms for the interbraided Regular Knots between the bight-boundaries 1_L and 2_L , respectively between the bight-boundaries 1_R and 2_R , are identical to those on pg. 1286.

Example 3.

Let in Fig. 1009 $C_1 = 15, C_2 = 13, C_3 = 15$, then for a component with such a first-return string-run $\beta = 4C_1 + 3C_2 = 4C_3 + 3C_2 = 99$ while $\alpha = 3$. Note that C_1, C_2 and C_3 must be chosen so that β is divisible by $\alpha = 3$. Let $B_c = 21$. Note that B_c must be chosen so that B_c is divisible by $\alpha = 3$.

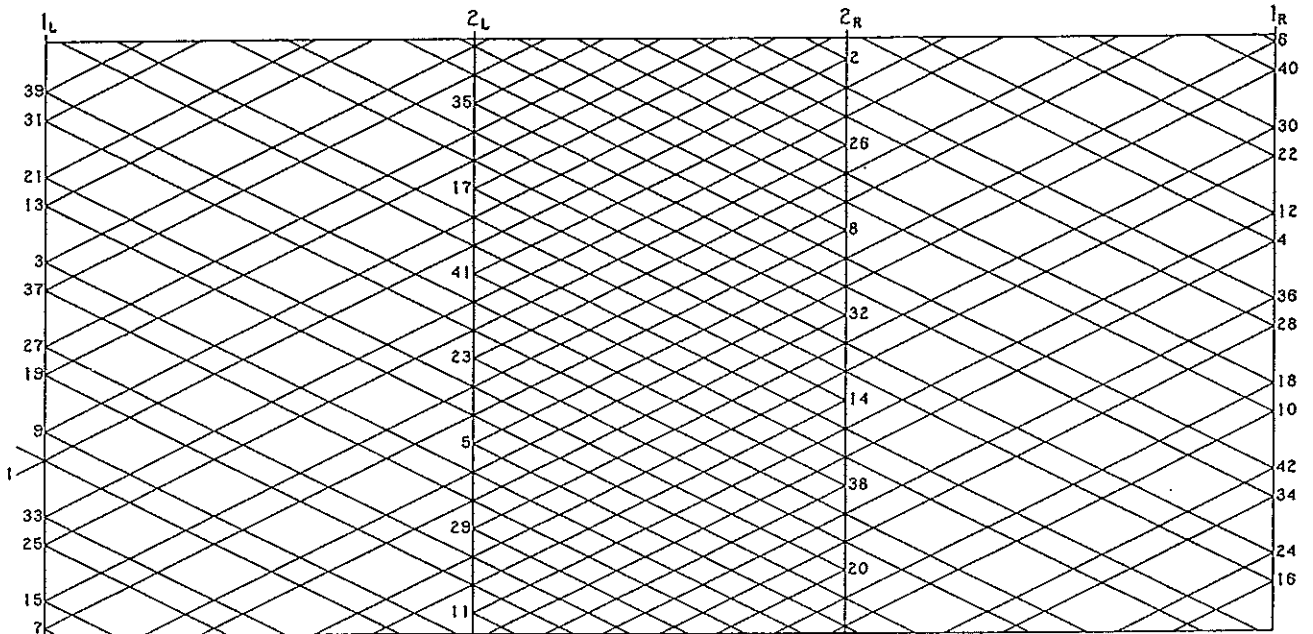


Fig. 1023 — The string-run of the foundation braid.

Thus for this component we obtain:

$$\lambda = \text{g.c.d.} \left(\frac{\beta}{\alpha}, \frac{B_c}{\alpha} \right) = \text{g.c.d.} \left(\frac{99}{3}, \frac{21}{3} \right) = \text{g.c.d.} (33, 7) = 1,$$

and hence only one essential string is required.

The string-run of this component consist of $\left(\frac{B_c}{\alpha} \right) = \left(\frac{21}{3} \right) = 7$ consecutive first-return string-runs.

The diagram in Fig. 1023 depicts the string-run of the foundation braid.

This foundation braid can be interbraided with two Regular Cylindrical Braids, one between the two leftmost bight-boundaries 1_L and 2_L and one between the two rightmost bight-boundaries 1_R and 2_R . For each of these two Regular Cylindrical Braids $p = 5$ and $b = 7$. Hence each braid is a Regular Knot and thus requires only one essential string.

Fig. 1024 depicts the string-runs of the two interbraided Regular Knots.

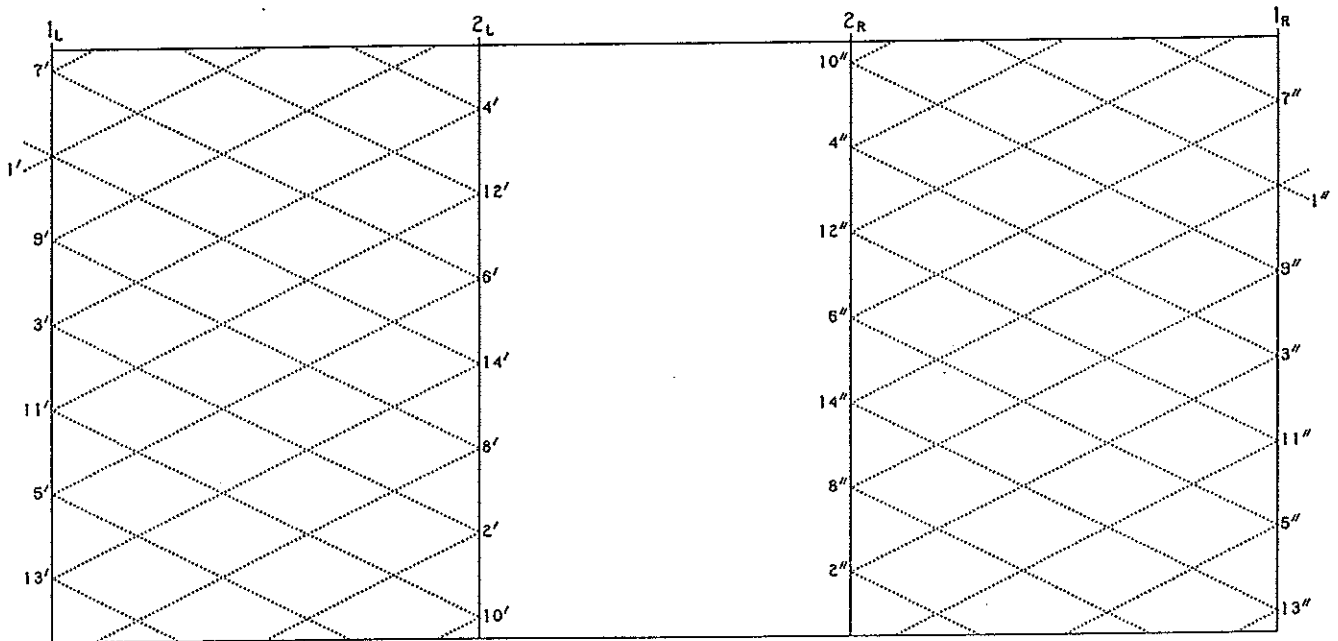


Fig. 1024 — The string-runs of the two interbraided Regular Knots.

A superimposed coding on the three string-runs is shown in Fig. 1025.

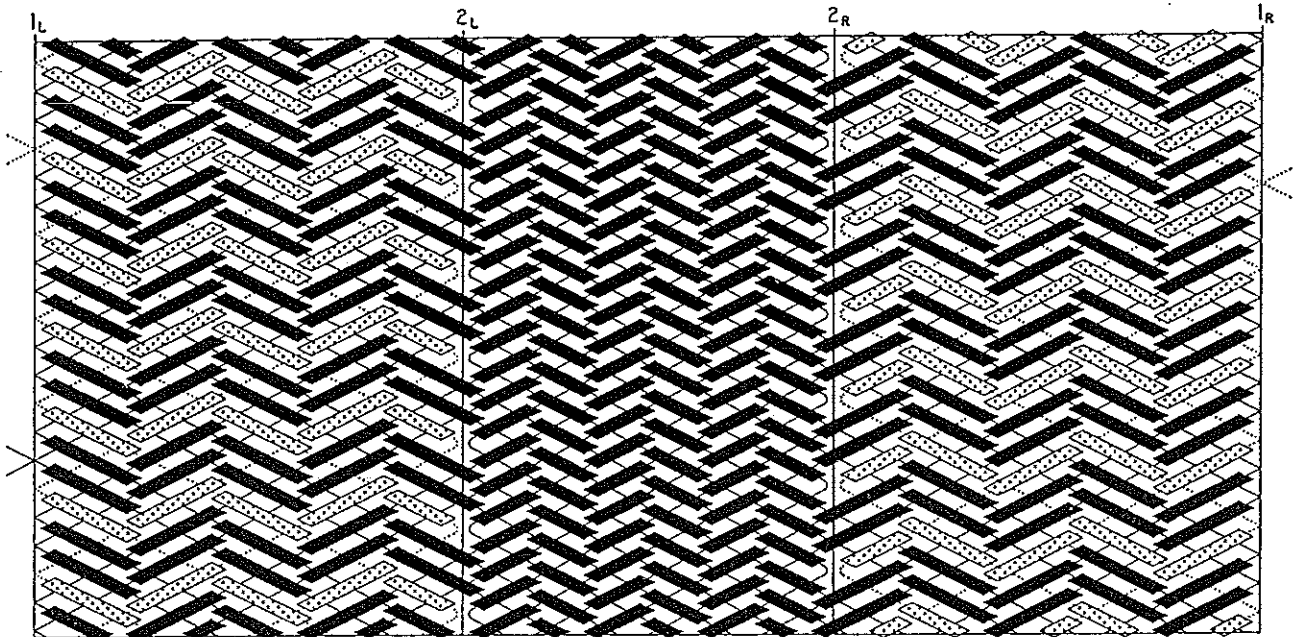


Fig. 1025 — A coding superimposed on the string-runs.

The half-cycle braiding algorithms for the foundation knot can be read from the tables in Figs. 1026 & 1027.

1. $1_L \rightarrow 2_R$: Free run.
2. $2_R \rightarrow 1_L$: o .
3. $1_L \rightarrow 1_R$: o .
4. $1_R \rightarrow 2_L$: o .
5. $2_L \rightarrow 1_R$: o .
6. $1_R \rightarrow 1_L$: $u - 3o$.

Euclid's algorithm, the path formula, the path in the RKT for the interbraided Regular Knots and their algorithm diagrams are shown in Fig. 1028.

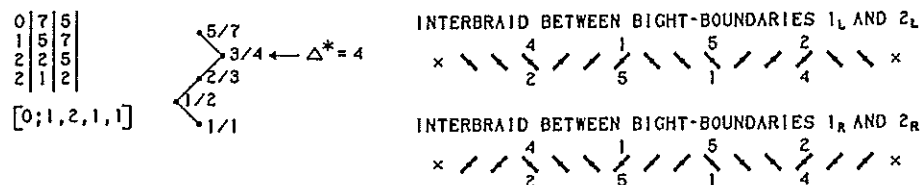


Fig. 1028 — Euclid's algorithm, path formula, path in RKT and algorithm diagrams for interbraided Regular Knots.

For the interbraided Regular Knot between the bight-boundaries 1_L and 2_L , the algorithm diagram is identical to the upper algorithm diagram in Fig. 1015, pg. 1282 and hence the half-cycle braiding algorithms for the interbraided Regular Knot between the bight-boundaries 1_L and 2_L are identical to the ones on pg. 1282.

The half-cycle braiding algorithms for the half-cycles $1''-14''$ of the interbraided Regular Knot between the bight-boundaries 1_R and 2_R are identical to the braiding algorithms for the half-cycles $1'-14'$ of the interbraided Regular Knot between the bight-boundaries 1_L and 2_L .

Example 4.

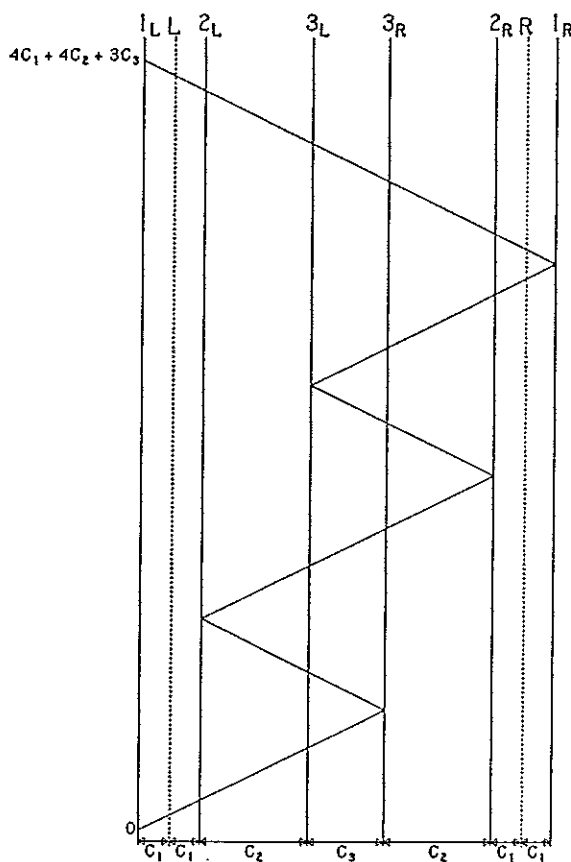


Fig. 1029 — The first-return string-run of a component in a cylindrical braid.

Let in Fig. 1029 $C_1 = 2$, $C_2 = 19$, $C_3 = 9$, then for a component with such a first-return string-run $\beta = 4C_1 + 4C_2 + 3C_3 = 4 \times 2 + 4 \times 19 + 3 \times 9 = 8 + 76 + 27 = 111$ while

$\alpha = 3$. Note that C_1, C_2 and C_3 must be chosen so that β is divisible by $\alpha = 3$. Let $B_c = 27$. Note that B_c must be chosen so that B_c is divisible by $\alpha = 3$.

Thus for this component we obtain:

$$\lambda = \text{g.c.d.} \left(\frac{\beta}{\alpha}, \frac{B_c}{\alpha} \right) = \text{g.c.d.} \left(\frac{111}{3}, \frac{27}{3} \right) = \text{g.c.d.} (37, 9) = 1,$$

and hence only one essential string is required.

The string-run of this component consist of $\left(\frac{B_c}{\alpha} \right) = \left(\frac{27}{3} \right) = 9$ consecutive first-return string-runs.

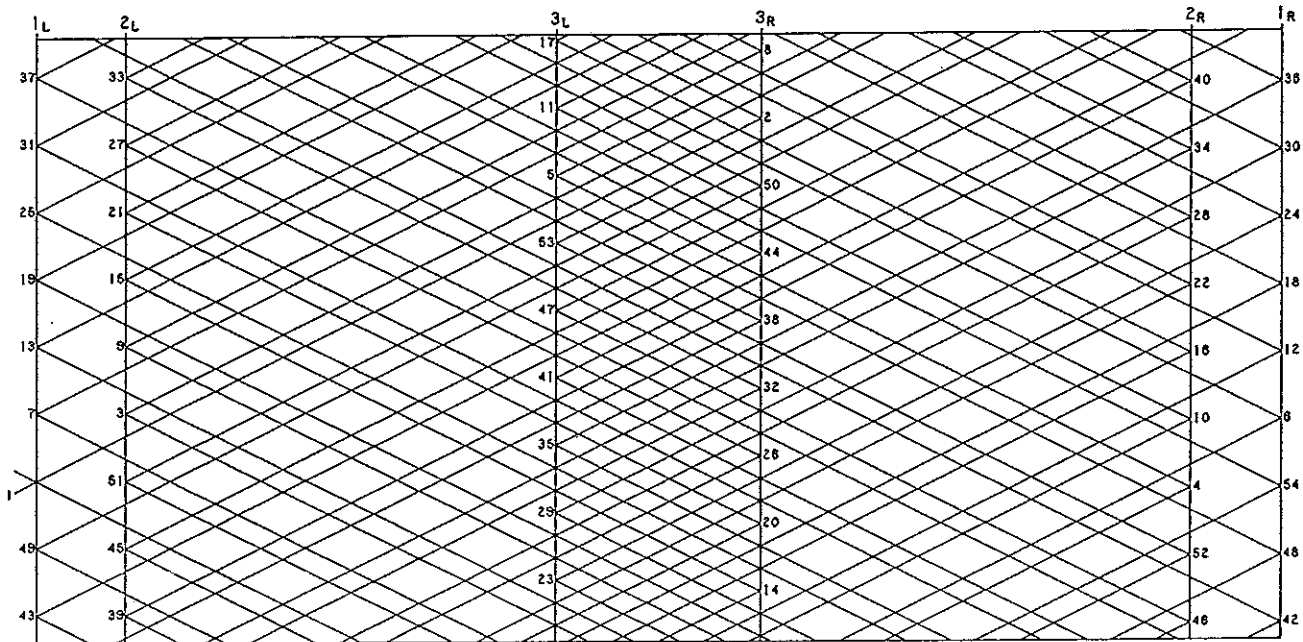


Fig. 1030 — The string-run of the foundation braid.

This foundation braid can be interbraided with two Regular Cylindrical Braids, one between bight-boundaries L and 3_L and one between bight-boundaries R and 3_R .

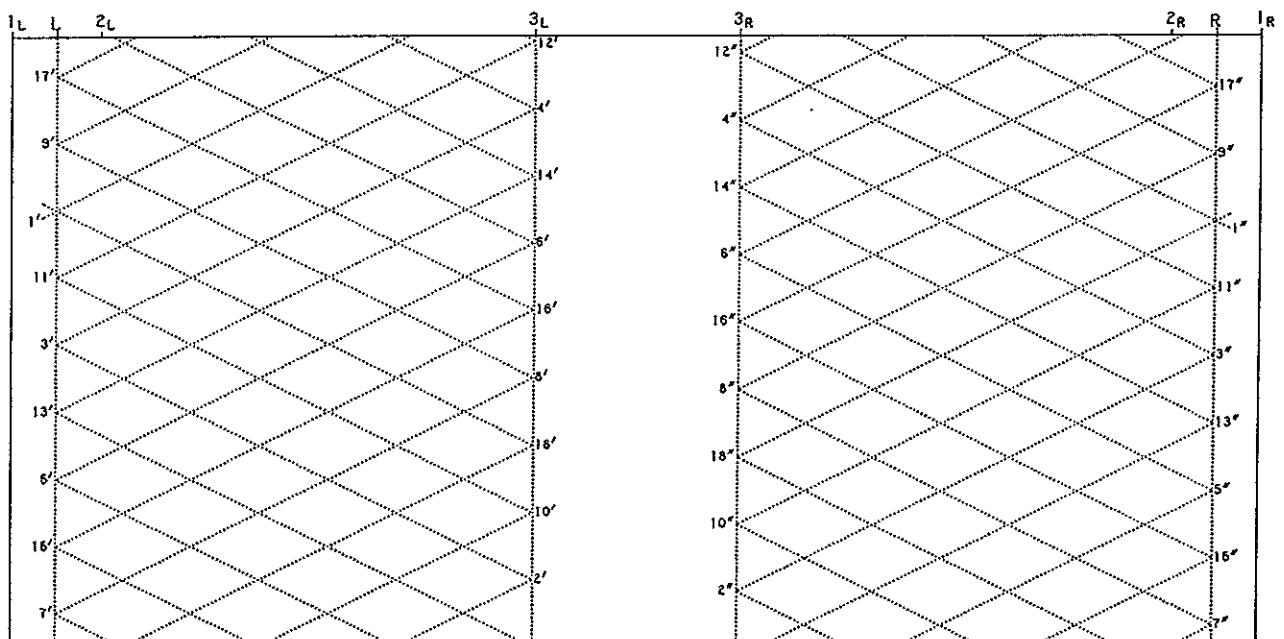


Fig. 1031 — The string-runs of the two interbraided Regular Knots.

Fig. 1030 depicts the string-run diagram of the foundation braid and in Fig. 1031 are depicted the string-runs of the two interbraided Regular Knots.

For each of these two Regular Cylindrical Braids $p = 7$ and $b = 9$. Hence each braid is a Regular Knot and thus requires only one essential string.

A superimposed coding on the three string-runs is shown in Fig. 1032.

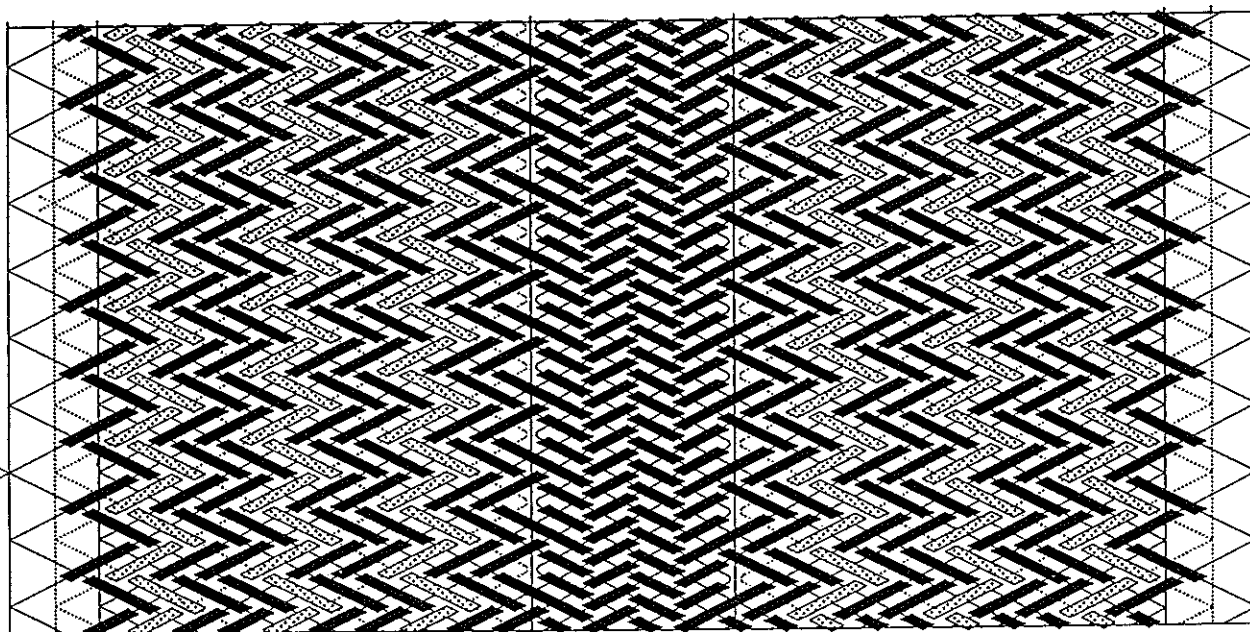


Fig. 1032 — A coding superimposed on the string-runs.

The half-cycle braiding algorithms for the foundation knot can be read from the tables in Figs. 1033 & 1034.

1. $1_L \rightarrow 3_R$: Free run.
2. $3_R \rightarrow 2_L$: u .
3. $2_L \rightarrow 2_R$: o .
4. $2_R \rightarrow 3_L$: $2o$.
5. $3_L \rightarrow 1_R$: $2o$.
6. $1_R \rightarrow 1_L$: $u - 2o - u$.
7. $1_L \rightarrow 3_R$: $o - u$.
8. $3_R \rightarrow 2_L$: $o - 2u$.
9. $2_L \rightarrow 2_R$: $o - u - o - u$.
10. $2_R \rightarrow 3_L$: $o - 2u - 2o$.
11. $3_L \rightarrow 1_R$: $u - 2o - u - o - u$.
12. $1_R \rightarrow 1_L$: $o - 2u - 4o - u$.
13. $1_L \rightarrow 3_R$: $u - 2o - u$.
14. $3_R \rightarrow 2_L$: $u - 2o - 2u$.
15. $2_L \rightarrow 2_R$: $2u - o - u - 2o - 2u$.
16. $2_R \rightarrow 3_L$: $2u - 2o - 2u - 2o$.
17. $3_L \rightarrow 1_R$: $2u - 3o - u - 2o - u$.
18. $1_R \rightarrow 1_L$: $u - 2o - 2u - 2o - 2u - 2o - u$.
19. $1_L \rightarrow 3_R$: $2o - u - 2o - u$.
20. $3_R \rightarrow 2_L$: $o - 2u - 2o - 2u$.
21. $2_L \rightarrow 2_R$: $o - 3u - o - u - o - u - 2o - 2u$.
22. $2_R \rightarrow 3_L$: $4u - 2o - 2u - 2o$.
23. $3_L \rightarrow 1_R$: $2u - 2o - u - o - 2u - 2o - u$.

- 52. $2_R \rightarrow 3_L : 2o - 2u - 2o - 2u - 2o - 4u - 2o - 2u - 2o.$
- 53. $3_L \rightarrow 1_R : 2u - 2o - u - 3o - 2u - 2o - 2u - 2o - 2u - 2o - u.$
- 54. $1_R \rightarrow 1_L : 2o - 2u - 2o - 2u - 2o - 2u - 2o - 2u - 2o - 2u - 3o - 2u - 2o - 2u - 2o - 2u - 2o - u.$

Euclid's algorithm, the path formula, the path in the RKT for the interbraided Regular Knots and their algorithm diagrams are shown in Fig. 1035.

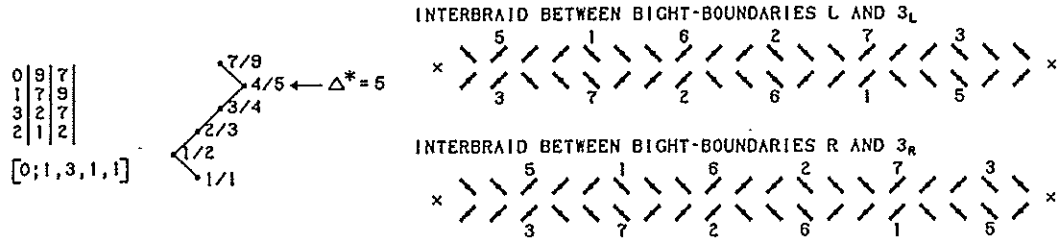


Fig. 1035 — Euclid's algorithm, path formula, path in RKT and algorithm diagrams for interbraided Regular Knots.

For the interbraided Regular Knot between the bight-boundaries L and 3_L we read the following half-cycle braiding algorithms from its algorithm diagram:

- 1'. $i = 0$: $u - 2o - 2u - 2o - 2u - 2o - 2u.$
- 2'. $(i = 0)$: $2u - 2o - 2u - 2o - 2u - 2o - u.$
- 3'. $(i = 0)$: $u - 2o - 2u - 2o - 2u - 2o - 2u.$
- 4'. $(i \leq 1)$: $2u - 2o - 3u - 2o - 2u - 2o - u.$
- 5'. $(i \leq 1)$: $u - 2o - 3u - 2o - 2u - 2o - 2u.$
- 6'. $(i \leq 2)$: $2u - 2o - 3u - 2o - 3u - 2o - u.$
- 7'. $(i \leq 2)$: $u - 2o - 3u - 2o - 3u - 2o - 2u.$
- 8'. $(i \leq 3)$: $2u - 2o - 3u - 2o - 3u - 2o - 2u.$
- 9'. $(i \leq 3)$: $u - 2o - 3u - 2o - 3u - 2o - 3u.$
- 10'. $(i \leq 4)$: $2u - 2o - 3u - 2o - 3u - 2o - 2u.$
- 11'. $(i \leq 4)$: $u - 2o - 3u - 2o - 3u - 2o - 3u.$
- 12'. $(i \leq 5)$: $2u - 3o - 3u - 2o - 3u - 2o - 2u.$
- 13'. $(i \leq 5)$: $u - 3o - 3u - 2o - 3u - 2o - 3u.$
- 14'. $(i \leq 6)$: $2u - 3o - 3u - 3o - 3u - 2o - 2u.$
- 15'. $(i \leq 6)$: $u - 3o - 3u - 3o - 3u - 2o - 3u.$
- 16'. $(i \leq 7)$: $2u - 3o - 3u - 3o - 3u - 3o - 2u.$
- 17'. $(i \leq 7)$: $u - 3o - 3u - 3o - 3u - 3o - 3u.$
- 18'. $(i \leq 8)$: $2u - 3o - 3u - 3o - 3u - 3o - 2u.$

The half-cycle braiding algorithms for the half-cycles 1''-18'' of the interbraided Regular Knot between the bight-boundaries R and 3_R are identical to the ones above for the half-cycles 1'-18' of the interbraided Regular Knot between the bight-boundaries L and 3_L .

Note the string-run of the right-hand interbraided knots with the '' half-cycles in Fig. 1011 (in association with Figs. 1012, 1016, 1017), in Fig. 1024 (in association with Fig. 1025), and in Fig. 1031 (in association with Fig. 1032). The placing of the Standing Ends obviously simplifies the half-cycle braiding algorithms involved — refer to *The Braider*, Issue No. 53, pg. 1245.